Mode-locking transitions in nanostructured weakly disordered lasers

L. Angelani,[1] C. Conti,[2,3] L. Prignano,[4] G. Ruocco,[3,4] and F. Zamponi[5]
[1]*Research Center SMC INFM-CNR, Università di Roma "La Sapienza," I-00185 Roma, Italy*
[2]*Centro Studi e Ricerche "Enrico Fermi," Via Panisperna 89/A, I-00184 Roma, Italy*
[3]*Research Center Soft INFM-CNR, Università di Roma "La Sapienza," I-00185 Roma, Italy*
[4]*Dipartimento di Fisica, Università di Roma "La Sapienza," I-00185 Roma, Italy*
[5]*Service de Physique Théorique, CEA Saclay, 91191 Gif sur Yvette Cedex, France*
(Received 1 December 2006; revised manuscript received 31 May 2007; published 15 August 2007)

We report on a statistical approach to mode-locking transitions of nanostructured laser cavities characterized by an enhanced density of states. We show that the equations for the interacting modes can be mapped onto a statistical model exhibiting a first-order thermodynamic transition, with the average mode energy playing the role of inverse temperature. The transition corresponds to a phase locking of modes. Extended modes lead to a mean-field-like model, while in the presence of localized modes, as due to a small disorder, the model has short-range interactions. We show that simple scaling arguments lead to observable differences between transitions involving extended modes and those involving localized modes. We link the thermodynamic transition to a topological singularity of the phase space, as previously reported for similar models. Finally, we solve the dynamics of the model, predicting a jump in the relaxation time of the coherence functions at the transition.

DOI: 10.1103/PhysRevB.76.064202 PACS number(s): 42.55.Ah, 05.70.Fh, 42.55.Zz

I. INTRODUCTION

Laser mode locking (ML) is well known in standard optical resonators, which are characterized by equispaced resonances.[1,2] ML in such a kind of system is a valuable route for the generation of ultrashort pulses, in particular, when it is "self-starting," as due to the nonlinear interaction between laser longitudinal modes.[3] Given the growing interest in high-Q microresonators and photonic crystals,[4,5] it is interesting to consider ML in integrated devices, which could trigger a new generation of highly miniaturized lasers emitting ultrashort pulses (see, e.g., Ref. 6).

In this respect, there is a remarkable difference between standard resonators and nanostructured cavities; indeed, the latter are characterized by a nonuniform distribution of resonances, given by a strongly modulated density of states (DOS).[5] This situation favors a formulation of the analysis of the self-mode-locking transition, based on a mean-field thermodynamic approach: this is the topic of the present paper, also including the effect of some disorder in the system. The thermodynamic approach to multimode interactions in various physical frameworks is well established.[7] For example, it was recently applied to transverse-mode interaction in resonators[8,9] as well as to standard-laser mode-locking transition.[10–12] This transition can be described in terms of an effective temperature T, which encompasses the level of noise due to spontaneous emission and the amount of energy stored into each mode. At high T, the mode phases are independent and rapidly varying ("free-run" or "paramagnetic phase"); conversely, either reducing the spontaneous emission noise or increasing the pumping rate, a low-temperature ("ferromagnetic") phase can be reached, corresponding to the mode phases locked at the same value. In the present paper, we use a statistical mechanics approach to describe the mode-locking transition, introducing a phase-dependent interacting Hamiltonian and discussing its scaling property and how it depends on the extended and/or localized nature of the involved lasing modes.

A paradigm that has been recently shown to be very effective for describing the nonlinear interaction of many "modes" and the resulting phase transitions and/or kinetic arrest is the potential energy landscape (PEL) approach (see, e.g., Refs. 13 and 14). The PEL, as a manifold in the configurational phase space, has many stationary points (typically minima and saddles),[15] whose distribution strongly affects the thermodynamics (and the dynamics) of the system. Recently, this paradigm, developed to investigate the glass transition phenomena, has been applied to the field of photonics, including optical solitons[16,17] and random lasers.[18,19] In this respect, it is worth to note that the geometrical interpretation of the laser threshold was recognized since the beginning of laser theory, and is considered as one of the successful applications of catastrophe theory, which classifies the singularities of multidimensional manifolds.[7,20] It is not surprising, therefore, that the mode-locking transition can be interpreted according to the thermodynamic and/or topological transition point of view. Extending the topological approach to the nanolaser is interesting for different reasons: on one hand, this provides an elegant and comprehensive theoretical framework to laser theory, and on the other hand, it can be relevant from a fundamental physical perspective.

In this respect, we also investigate here the link between thermodynamic properties (the presence of phase transitions and their order) and topological changes of the energy hypersurface. Indeed, in recent years a "topological hypothesis"[21,22] has been suggested to hold for systems undergoing thermodynamic phase transitions: the latter are supposed to be manifestation of topological discontinuities of certain submanifolds in configuration space. Subsequently, this topological hypothesis has been formalized in a theorem for a strict class of systems, described by smooth, bounded below, confining, and finite-range potentials: a topology change is a necessary condition for the appearance of a phase transition.[23–25] Many works have been devoted to the study of solvable model systems in order to test the correctness of the above hypothesis and/or theorem,[26–30] obtaining a variety of results (for a recent review, see Ref. 31). However, it is worth noting that many of the analyzed models do not fulfill the hypotheses of the theorem (being long range, not confin-

ing, or not smooth). Also, the multimode laser model we study in this paper does not fulfill the above hypotheses. However, by analytically analyzing the topology of the energy hypersurface, we find that the topological hypothesis is verified, finding a topological change at the same energy at which a phase transition take places.

Finally, we report on the dynamics of the lasing modes. We are able to give explicit expressions of the single-mode and multimode first-order coherence functions of the laser emission. Our analysis predicts a jump in the relaxation time (and correspondingly in the laser linewidth) at the mode-locking transition. The scaling properties of the threshold average mode energy at the transition are found to be strongly sensible to the degree of localization of the involved modes.

The outline of this paper is as follows: In Sec. II, we will recall the mode-coupling approach to multimode lasers. In Sec. III, we will discuss the physical signatures of transitions involving either localized or delocalized modes. In Sec. IV, we will report on the thermodynamic approach. The analysis of the topological origin of the laser transition is given in Sec. V. In Sec. VI, we discuss the dynamics of the model, focusing on measurable correlation functions. Conclusions are drawn in Sec. VII.

II. MULTIMODE LASER EQUATIONS

The coupled-mode theory equations in a nonlinear cavity can be written in the form[11,19,32–34]

$$\frac{da_s}{dt} = -\frac{\partial H_I}{\partial a_s^*} - \alpha_s a_s(t) + [\gamma_s - g_s|a_s(t)|^2]a_s(t) + \eta_s(t)$$
$$= -\frac{\partial \mathcal{H}}{\partial a_s^*} + \eta_s(t), \tag{1}$$

with

$$\mathcal{H} = H_o + H_I, \tag{2}$$

and

$$H_o = \sum_s (\alpha_s - \gamma_s)|a_s|^2 + \frac{1}{2}g_s|a_s|^4 = \sum_s V_s(a_s). \tag{3}$$

In Eq. (1), $s=1,2,\ldots,N$ with N the total number of modes, while a_s is the complex amplitude of the mode at ω_s, such that $\mathcal{E}_s=\omega_s|a_s|^2$ is the energy stored in the mode. Radiation losses and material absorption are represented by the coefficient α_s, while $\gamma_s - g_s|a_s|^2$ represents the saturable gain term and, as usual, the quantum noise term due to spontaneous emission is given by a random term η_s such that $\langle \eta_s(t)\eta_p(t')\rangle = 2k_B T_{bath}\delta_{sp}\delta(t-t')$, where k_B is the Boltzmann constant and T_{bath} is an effective temperature.[19] The nonlinear interaction term is

$$H_I = \mathrm{Re}\left[\frac{1}{4}\sum_{\{spqr\}} g_{spqr}a_s a_p a_q^* a_r^*\right], \tag{4}$$

where the sum is extended over all mode resonances such that $\omega_s+\omega_p=\omega_q+\omega_r$. The term $s=p=q=r$ is not included as it is already described by g_s; the Hamiltonian H_I describes mode interaction due to the nonlinearity of the gain medium. The field overlap is given by

$$g_{spqr} = \frac{\sqrt{\omega_s\omega_p\omega_q\omega_r}}{2i}\int_V \chi_{\alpha\beta\gamma\delta}(\omega_s;\omega_q,\omega_r,-\omega_p,\mathbf{r})$$
$$\times E_s^\alpha(\mathbf{r})E_p^\beta(\mathbf{r})E_q^\gamma(\mathbf{r})E_r^\delta(\mathbf{r})dV, \tag{5}$$

where V is the cavity volume, χ is the third-order susceptibility tensor due to the resonant medium, and E_p^α are the components ($\alpha=1,2,3$) of the vectorial mode of the cavity at the resonance ω_p. χ is given, in the simplest formulation, by the Lamb theory[32,33] and, neglecting mechanisms like self- and cross-phase modulation (which give phase-independent contribution to the relevant Hamiltonian, see below), can be taken as real valued; under standard approximations, the tensor g is a quantity symmetric with respect to the exchange of any couple of indexes.

By letting $a_s(t)=A_s(t)\exp[i\varphi_s(t)]$, the $\mathcal{H}$ can be rewritten as

$$\mathcal{H}(G,\varphi) = H_o + \sum_{\{spqr\}} G_{spqr}\cos(\varphi_s+\varphi_p-\varphi_q-\varphi_r), \tag{6}$$

where $H_o=\Sigma_s V_s(A_s)$ only depends on the amplitudes and $G_{spqr}=2g_{spqr}A_sA_pA_qA_r$. As discussed in the literature,[11] Eqs. (1) are Langevin equations for a system of N particles moving in $2N$ dimensions and the invariant measure is given by $\exp(-\mathcal{H}/k_BT_{bath})$.

In a standard laser, the resonant frequencies are equispaced and this gives rise to various formulations of laser thermodynamics, which are based on the fact that the $\omega_s+\omega_p=\omega_q+\omega_r$ will only involve a limited number of interacting modes.[10,11] The situation is drastically different for nanostructured systems displaying a photonic band gap. It is indeed well established that in proximity of the band edge, a DOS enhancement with respect to vacuum is obtained. All the corresponding modes will have overlapping resonance such that $\omega_s \cong \omega_0$, (where ω_0 is the position of the peak in the density of states, which is assumed to be in correspondence of the resonance of the amplifying atomic medium); additionally, the resonance condition $\omega_s+\omega_p=\omega_q+\omega_r$ need not be exactly satisfied, but it is sufficient that the linewidth of the corresponding modes needs to be overlapped for a relevant interaction.[36] Hence, for such a kind of system, it is interesting to consider a mean-field regime where all the modes interact in a limited spectral region around ω_0. For the mode-locking transition, one can limit to consider the phase dynamics. Indeed, ML entails the passage from a regime in which the mode phases are independent and rapidly varying (free-run regime or paramagnetic phase in the following)[32] on times scales of the order of 10 fs (Ref. 37) to a regime in which they are all locked at the same values (ferromagnetic phase). In correspondence of this transition, the laser output switches from a continuous wave noisy emission to a highly modulated signal (which is a regular train of short pulses for equispaced resonances). Mode-amplitude dynamics is not affected (at the first approximation) by the onset of ML. Indeed, for lasing modes $\gamma_s > \alpha_s$, so that the potential $V_s(A_s)$

(entering in the equations for the A_s variables) has a single minimum at $A_s^o = \sqrt{(\gamma_s - \alpha_s)/g_s}$. Provided that the potential well is deep enough, i.e., the V_s term dominates with respect to the thermal noise η_s and the interaction term H_I, we can treat the dynamics of the A_s variables as small fluctuations around the minimum. As zero-order approximation, we can neglect these fluctuations and consider the A_s as *quenched* variables $[A_s(t) \simeq A_s^o \simeq A$, having neglected also the mode dependence of loss and/or gain terms in $H_o]$. Within the above approximations, the relevant subspace spanned by the system is then given by the phases that are taken as the dynamic variables (see, for example, Ref. 1 for a discussion of the role of mode phases with respect to amplitudes in ML processes).

III. LOCALIZED VERSUS DELOCALIZED MODES IN THE SELF-MODE-LOCKING TRANSITION

In previous works,[18,19] we made reference to a completely random resonator, for which the G coefficients were taken Gaussian distributed with zero mean. This is the natural approach when dealing with strongly disordered resonators, in which the involved modes can be localized or delocalized in the structure and the corresponding resonances and spatial distribution can have different degrees of overlaps (as in Refs. 38–40). Here, we make reference to the opposite regime, corresponding to the case in which the structure is quasiordered, with the presence of a small amount of disorder. The disorder is such that the variations in the coupling coefficients g_{spqr} can be taken as negligible with respect to their statistical average $\langle g_{spqr} \rangle \simeq g$; however, it is sufficient to induce the existence of a tail of localized modes in the photonic band gap.[41]

As discussed above, we consider mode resonances packed in a small spectral region $\Delta\omega$ (if compared with the central carrier angular region, i.e., $\Delta\omega \ll \omega_0$). This kind of system is very different from the standard laser cavity, with equispaced mode frequencies. A prototypical structure is given by a photonic crystal doped by active materials. In the absence of disorder, the involved modes are Bloch modes, which are extended over the whole sample and are absent in the forbidden band gap. Their DOS is peaked at the band-gap edge.[5] In this case, the modes have overlapping resonances (the width of each spectral line being determined by material and radiation losses) and they also have non-negligible spatial overlap (with exception of those mode combinations which are vanishing for symmetry reasons). In the presence of a small amount of disorder, it is well established[41] that a tail of localized states appears in the photonic band gap. Hence, the localized states also have overlapping resonances in tiny spectral regions in proximity of the band edge. Their spatial overlap can be strongly reduced with respect to the Bloch modes; however, the exponential tails of their spatial profiles are expected to provide nonvanishing values for g. Localized states can also be introduced intentionally, e.g., by using defects in a planar photonic crystal slab waveguide[4] or in coupled cavity systems (see, e.g., Ref. 6 and references therein). In this case, the spatial overlap and the resonance frequencies can be tailored at will. Thus, in the general case, extended and localized states can be involved in the mode-locking transitions here considered. However, simple scaling arguments lead to the conclusion that the two kinds of modes display a macroscopic difference in their "thermodynamics."

Extended modes. We start with considering the extended modes. From the normalization, the modules of the eigenvectors E_s are such that $\int dV |E_s|^2 = \text{const}$. As a consequence, denoting with V_o the volume over which a given mode is different from zero, one has $E_s(\mathbf{r}) \sim V_o^{-1/2}$. For extended modes, $V_o \propto V$ and most of the modes are spatially overlapped, hence the coupling in Eq. (5) is different from zero for all quadruples of modes and the sum in Eq. (6) involves all the modes (within the spectral region $\Delta\omega$). In the absence of strong disorder, the coupling is almost independent of the quadruple of modes involved, $g_{spqr} \cong g$. Given that $|E_s(\mathbf{r})|^4 \sim V^{-2}$, as stated above, and that $\chi(\mathbf{r}) \sim \text{const}$ (i.e., in the absence of strong disorder, the local susceptibility will have small fluctuations around its average), we get from Eq. (5)

$$g \sim \int_V \chi(\mathbf{r}) |E_s(\mathbf{r})|^4 dV \propto V^{-1} \propto N^{-1}, \tag{7}$$

as the number of modes is proportional to the volume. Considering the fact that the sum in Eq. (6) is over N^4 terms, one obtains that $H_I \propto N^3$: the Hamiltonian is hence more than extensive (for an extensive one, $H \propto N$). However, a thermodynamics approach is still possible if one accepts that the effective temperature will depend on the volume: the effective temperature will be taken as proportional to $N^{-2} \propto V^{-2}$, as detailed below, so that the resulting effective Hamiltonian will be proportional to V. Physically, this corresponds to the fact that the energy (and hence the pumping rate) needed to induce the ML transition will grow with the number of modes, if only extended modes are involved. In conclusion, considering the invariant measure (denoting $A_s \simeq A$, $g_{spqr} \simeq g$, and $G_{spqr} \simeq G = gA^4$), one has

$$\begin{aligned} \exp\left(-\frac{H_I}{k_B T_{bath}}\right) &= \exp\left[-\frac{gA^4}{k_B T_{bath}} \sum_{spqr} \cos(\varphi_s + \varphi_p - \varphi_q - \varphi_r)\right] \\ &= \exp\left[-\frac{gA^4 N^3}{k_B T_{bath}} \frac{1}{N^3} \sum_{spqr} \cos(\varphi_s + \varphi_p - \varphi_q - \varphi_r)\right] \\ &\equiv \exp[-\beta H^{(ext)}], \end{aligned} \tag{8}$$

where $\beta \equiv |g| A^4 N^3 / k_B T_{bath} \equiv 1/T \propto N^2$ is an inverse adimensional temperature, and the mode-phase-dependent (extensive) Hamiltonian is given by (within an irrelevant additive term)

$$H^{(ext)} = \frac{1}{N^3} \sum_{spqr} [1 - \cos(\varphi_s + \varphi_p - \varphi_q - \varphi_r)]. \tag{9}$$

In Eq. (9), we have used the fact that $g < 0$ in all the physically relevant regimes. No transition is expected for $g > 0$ (corresponding to "antiferromagnetic" interactions), as detailed below. Note that as we assumed that the condition $\omega_s + \omega_p = \omega_q + \omega_r$ is not exactly satisfied, and possibly due to the presence of disorder, the integrand in Eq. (5) might have

oscillations or fluctuations in sign that can affect the scaling of g with volume (the case of completely random fluctuations leads to a scaling $g \propto V^{-3/2}$ and to an extensive Hamiltonian as in Refs. 18 and 19). Intermediate regimes might be present depending on the strength of the disorder.

Localized modes. Next, we consider localized modes, that exponentially decay in space. Defining V_o as above, it turns out that it does not scale with the volume V of the sample, but can be written as $V_o = L_o^3$, where L_o is an average localization length. The overlap coefficients g_{spqr} will be nonzero only if the quadruples of modes *spqr* have large spatial overlap, i.e., they are "neighbors in space." The integral in Eq. (5) is over the region where all the four modes are nonvanishing, which is a finite region that does not depend on V: therefore, the couplings g_{spqr} are independent of the volume in this case. Hence, the sum in the Hamiltonian will only involve first neighbors and $H_I \propto V$, as is usual for a short-range interaction. For the invariant measure, we will have (the angular bracket in $\langle spqr \rangle$ denoting sum over first neighbors)

$$\exp\left(-\frac{H_I}{k_B T_{bath}}\right) = \exp\left[-\frac{gA^4}{k_B T_{bath}} \sum_{\langle spqr \rangle} \cos(\varphi_s + \varphi_p - \varphi_q - \varphi_r)\right] = \exp[-\beta H^{(loc)}], \tag{10}$$

where $\beta \equiv |g|A^4/k_B T_{bath} \equiv 1/T$ will not depend on the system size (we stress that the system size must be such that a large number of localized modes are present), and the Hamiltonian (within irrelevant additive constants) is

$$H^{(loc)} = \sum_{\langle spqr \rangle} [1 - \cos(\varphi_s + \varphi_p - \varphi_q - \varphi_r)]. \tag{11}$$

Summarizing, if the transition involves extended modes, the effective temperature for the critical transition is expected to depend on the size of the system; conversely, for localized modes the critical temperature will be independent of the system size.

Unfortunately, at variance with fully connected (or "mean field") models as Eq. (9), analytical treatment of short-range Hamiltonians as Eq. (11) is almost always impossible and the analysis can only be numerically performed. However, it is well established within the statistical physics community that mean-field models obtained from first-neighbor systems conserve most of the thermodynamics properties, and more specifically, the existence of a thermodynamic transition, at least above the so called "lower critical dimension" d_l (for example, for the Ising model $d_l=1$, for the XY model $d_l=2$). Our model falls into the class of XY models, so we expect that the transition exists as long as $d>2$, also in the case of localized modes, and the following analysis applies at least qualitatively. Since Eq. (9) can be analytically treated for thermodynamic, topological, and dynamic properties, we will limit to this model in the following. The existence of a thermodynamic and/or topological transition is expected in the general case, while the different scaling properties of the effective temperature enable one to discern localized and delocalized interactions.

IV. THERMODYNAMICS

In this section, we study the thermodynamics of the laser Hamiltonian in the mean-field approximation [Eq. (9)], within the quenched amplitude approximation. The partition function is

$$Z = \int d\varphi e^{-\beta H(\varphi)}, \tag{12}$$

where H is

$$H = \frac{1}{N^3} \sum_{spqr} [1 - \cos(\varphi_s + \varphi_p - \varphi_q - \varphi_r)]. \tag{13}$$

The Hamiltonian (13) is very similar to that defining the k trigonometric model for $k=4$, introduced in Ref. 30 with the aim of studying the relation between phase transitions and topological property of the potential energy surface.[22,42,43]

Defining the "magnetization"

$$z = \frac{1}{N} \sum_s e^{i\varphi_s} = \xi e^{i\psi}, \tag{14}$$

where ξ and ψ depend on $\{\varphi_s\}$, we have

$$H = \mathrm{Re}\left[\frac{1}{N^3} \sum_{spqr} [1 - \exp i(\varphi_s + \varphi_p - \varphi_q - \varphi_r)]\right] = \mathrm{Re}\left[\frac{1}{N^3} N^4 (1 - z^2 z^{*2})\right] = N(1 - \xi^4). \tag{15}$$

By definition, a vanishing z denotes uncorrelated phase, as in the free-run regime; conversely, if $z \neq 0$ the phases of the modes are correlated and locked. The thermodynamics of the mean-field model is exactly solved by neglecting the correlations between different degrees of freedom and obtaining an effective Hamiltonian that contains a parameter to be determined self-consistently. Introducing the mean (complex) magnetization $\zeta = \langle e^{i\varphi} \rangle$ and substituting in Eq. (13) the expression

$$\begin{aligned} e^{j(\varphi_s + \varphi_p - \varphi_q - \varphi_r)} \longrightarrow\ & e^{j\varphi_s} \langle e^{j\varphi_p} \rangle \langle e^{-j\varphi_q} \rangle \langle e^{-j\varphi_r} \rangle \\ & + \langle e^{j\varphi_s} \rangle e^{j\varphi_p} \langle e^{-j\varphi_q} \rangle \langle e^{-j\varphi_r} \rangle \\ & + \langle e^{j\varphi_s} \rangle \langle e^{j\varphi_p} \rangle e^{-j\varphi_q} \langle e^{-j\varphi_r} \rangle \\ & + \langle e^{j\varphi_s} \rangle \langle e^{j\varphi_p} \rangle \langle e^{-j\varphi_q} \rangle e^{-j\varphi_r} \\ & - 3 \langle e^{j\varphi_s} \rangle \langle e^{j\varphi_p} \rangle \langle e^{-j\varphi_q} \rangle \langle e^{-j\varphi_r} \rangle \\ =\ & 2\zeta\zeta^* (e^{j\varphi} \zeta^* + e^{-j\varphi} \zeta) - 3\zeta^2 \zeta^{*2} \\ =\ & 4\zeta^3 \cos\varphi - 3\zeta^4, \end{aligned} \tag{16}$$

where the last equality stands because we have chosen ζ to be real without loss of generality (corresponding to choosing a particular magnetization of the low-temperature state), the effective Hamiltonian h per degree of freedom reads as

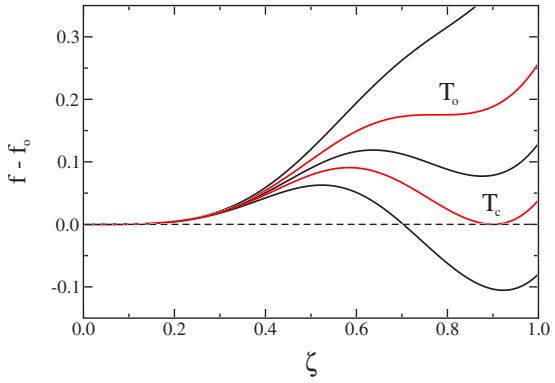

FIG. 1. (Color online) Free energy $f(\zeta)-f(\zeta=0)$ as a function of magnetization ζ at different temperatures. From high to low: $T=0.910$, $T_o=0.717$, $T=0.616$, $T_c=0.548$, and $T=0.504$. T_o marks the appearance of the unstable minimum, and T_c is the transition temperature at which the solution with $\zeta>0$ becomes thermodynamically stable.

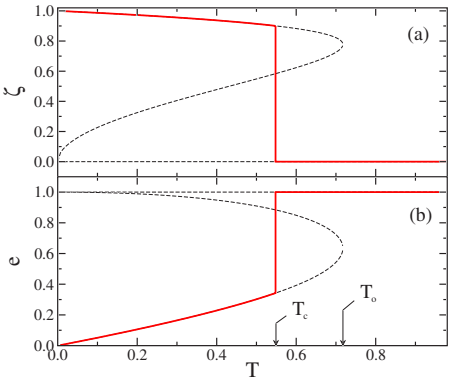

FIG. 2. (Color online) (a) Magnetization ζ and (b) energy e as a function of temperature. Full lines correspond to the thermodynamically stable solution of Eq. (18), whereas dashed lines are the unstable solutions. At $T_c=0.548$, a first-order thermodynamic phase transition takes place, while at $T_o=0.717$ unstable solutions appear.

$$h(\varphi) = 1 + 3\zeta^4 - 4\zeta^3 \cos\varphi. \tag{17}$$

The self-consistent equation for ζ turns out to be

$$\zeta = \langle \cos\varphi \rangle_h = \frac{I_1(4\beta\zeta^3)}{I_0(4\beta\zeta^3)}, \tag{18}$$

where $I_0(\alpha)=(2\pi)^{-1}\int_0^{2\pi} d\varphi \exp(\alpha\cos\varphi)$ and $I_1(\alpha)=I_0'(\alpha)$ are the modified Bessel function of order 0 and 1, and $\langle\cdots\rangle_h$ is the average over the probability distribution

$$P(\varphi) = \frac{e^{-\beta h(\varphi)}}{\mathcal{Z}}, \tag{19}$$

with

$$\mathcal{Z} = \int_0^{2\pi} d\varphi e^{-\beta h(\varphi)} = 2\pi e^{-\beta(1+3\zeta^4)} I_0(4\beta\zeta^3). \tag{20}$$

The solutions of Eq. (18) are the extrema of the free energy f as a function of ζ,

$$\beta f = -\ln \mathcal{Z} = \beta(1+3\zeta^4) - \ln 2\pi I_0(4\beta\zeta^3), \tag{21}$$

whose absolute minimum is the thermodynamical stable solution.

The value $\zeta=0$, corresponding to the paramagnetic solution, always solves Eq. (18), but it gives the stable (lower free energy) solution only for low β (high T). On lowering T, at $T_o=0.717$ other solutions appear such that $\zeta\neq 0$. However, the stable solution is still the paramagnetic one $\zeta=0$. At $T_c=0.548$, the solution $\zeta\neq 0$ becomes the stable one, and a first-order phase transition takes place. In Fig. 1, the ζ dependence of the free energy f is reported for different temperatures. The stable solution $\zeta(T)$ is shown in Fig. 2(a) (full line), while dashed lines denote unstable solutions (local minimum and maximum). In Fig. 2(b), the T dependence of the energy,

$$e = -\frac{\partial}{\partial\beta}\ln\mathcal{Z} = 1 - \zeta^4, \tag{22}$$

is shown for the stable (full line) and unstable (dashed lines) solutions.

A remark on the sign of the coupling g is as follows. For $g>0$, the sign of the cosine term in the Hamiltonian (13) is positive and the self-consistent equation reads $\zeta=-I_1(\beta\Delta 4\zeta^3)/I_0(\beta\Delta 4\zeta^3)$, which has the only solution $\zeta=0$. Then, in this case the phase transition does not take place.

V. TOPOLOGY

After having ascertained the existence of a first-order phase transition, we consider the property of the stationary points (saddles) of the potential energy landscape of the system.[30] As said in the Introduction, in recent works,[22,23] it has been conjectured that phase transitions are signaled by discontinuities in the configuration space topology. More precisely, for a system defined by a continuous potential energy function $V(q)$ (q denotes the N-dimensional vector of the generalized coordinates), a thermodynamic phase transition occurring at T_c (corresponding to energy V_c) is the manifestation of a topological discontinuity taking place at V_c (topological hypothesis). Such a connection has been proven to hold for smooth, confining, bounded below, and finite-range potentials.[23–25] For this class of systems, a topology change is a necessary condition for the appearance of a phase transition. The most striking consequence of this hypothesis is that the signature of a phase transition is present in the topology of the configuration space independent of the statistical measure defined on it. Through the Morse theory, topological changes are related to the presence of stationary points of V and, more specifically, to the discontinuous behavior of invariant quantity defined on them, as the Euler characteristic χ. Subsequent works[44,45] have shown that, at least for some model system, a *weak topological hypothesis* applies in place of the *strong* one: the V_θ at which a topological transition takes place does not coincide with the ther-

modynamic one, $V_c \neq V_\theta$, but is related to it by a saddle map M, from equilibrium energy level to stationary point energy $[M(V_c)=V_\theta]$. Then, the role of saddles has been demonstrated to be of high relevance for the topological interpretation of thermodynamic transitions. Here, we report on the saddle properties of the considered nanolaser model.

The stationary points $\bar{\varphi}$ are defined by the condition $dH(\bar{\varphi})=0$ and their order is defined as the number of negative eigenvalues of the Hessian matrix $H_{ij}=(\partial^2 H/\partial\varphi_i\partial\varphi_j)|_{\bar{\varphi}}$. To determine the location of stationary point, we have to solve the system

$$\frac{\partial H}{\partial \varphi_k} = 4\xi^3 \sin(\varphi_k - \psi) = 0, \quad \forall\, k, \tag{23}$$

where we have used Eqs. (14) and (15).

A first group of solutions arises for $\xi=0$; from Eq. (15), we have $H=N(1-\xi^4)$, and then the stationary points with $\xi(\bar{\varphi})=0$ are located at the energy $e=H(\bar{\varphi})/N=1$. Now, we restrict ourselves to the region $e\neq 1$ because, as we will see at the end, the quantities in which we are interested are singular when $e=1$. For $e\neq 1$, Eq. (23) becomes

$$\sin(\varphi_k - \psi) = 0, \quad \forall\, k, \tag{24}$$

and its solutions are

$$\varphi_k = [\psi + m_k \pi]_{\mathrm{mod}\ 2\pi}, \tag{25}$$

where $m_k=\{0,1\}$. The unknown constant ψ is found by substituting Eq. (25) in the self-consistency equation

$$z = \xi e^{i\psi} = N^{-1}\sum_i e^{i\varphi_i} = N^{-1}\sum_i e^{i(\psi+m_i\pi)} = N^{-1}e^{i\psi}\sum_i (-1)^{m_i}. \tag{26}$$

Introducing the quantity $n(\bar{\varphi})$ defined by

$$n = N^{-1}\sum_i m_i, \quad 1-2n = N^{-1}\sum_i (-1)^{m_i}, \tag{27}$$

we have, from Eq. (26),

$$\xi = 1-2n. \tag{28}$$

As ξ is positive defined, the only solutions are for $n<1/2$: there are no stationary points with $n>1/2$. For $n<1/2$, ψ can assume all the values in $[0,2\pi)$ for any choice of the set $\{m_k\}$ and all the stationary points of energy $e\neq 1$ have the form

$$\bar{\varphi}_k^{\mathbf{m}} = [\psi + m_k\pi]_{\mathrm{mod}\ 2\pi}, \quad \mathbf{m}=\{m_k\}, \quad m_k=(0,1) \tag{29}$$

under the condition

$$n = N^{-1}\sum_k m_k < 1/2.$$

The Hessian matrix is given by

$$H_{ij} = 4\xi^2\left\{-\frac{4}{N}\xi^2 \sin(\varphi_i-\psi)\sin(\varphi_j-\psi) - \frac{1}{N}\cos(\varphi_i-\varphi_j) + \delta_{ij}\xi\cos(\varphi_i-\psi)\right\}. \tag{30}$$

In the thermodynamic limit, it becomes diagonal,

$$H_{ij} \simeq 4\xi^3\delta_{ij}\cos(\varphi_i-\psi). \tag{31}$$

Neglecting the off-diagonal contributions (their contribution changes the sign of at most one of the N eigenvalues[30]), the eigenvalues λ_k of the Hessian calculated at the stationary point $\bar{\varphi}$ are obtained substituting Eq. (29) into Eq. (31),

$$\lambda_k = (-1)^{m_k} 4\xi^3. \tag{32}$$

Therefore, the stationary point order $\nu(\bar{\varphi})$, defined as the number of negative eigenvalues of the Hessian matrix, is simply the number of $m_k=1$ in the set $\mathbf{m}$ associated with $\bar{\varphi}$; we can identify the quantity $n(\bar{\varphi})$ given by Eq. (27) with the fractional order $\nu(\bar{\varphi})/N<1/2$ of $\bar{\varphi}$. Then, from Eqs. (15) and (28), we get a relation between the fractional order $n(\bar{\varphi})$ and the potential energy $e(\bar{\varphi})=H(\bar{\varphi})/N$ at each stationary point $\bar{\varphi}$. It reads

$$n = \frac{1}{2}[1-(1-e)^{1/4}], \tag{33}$$

where we have used the condition $n<1/2$. Equation (33) brings the condition

$$1-e>0, \tag{34}$$

so there are no stationary points for $e>1$, while for $e<1$ the fractional order $n=\nu/N$ of the stationary points is a well defined monotonic function of their potential energy e, given by Eq. (33).

The number of stationary points of a given order (apart from a degeneracy factor) is proportional to the number of ways in which one can choose ν times 1 among the $\{m_k\}$, i.e., $\binom{N}{\nu}$. Following Ref. 30, its logarithm,

$$\sigma(e) = \lim_{N\to\infty}\frac{1}{N}\ln\binom{N}{Nn(e)} = -n(e)\ln n(e) - [1-n(e)]\ln[1-n(e)], \tag{35}$$

represents the *configurational entropy* of the saddles. Substituting in this expression Eq. (33), we have

$$\sigma(e) = -\frac{1}{2}[1-(1-e)^{1/4}]\ln\left\{\frac{1}{2}[1-(1-e)^{1/4}]\right\} - \frac{1}{2}[1+(1-e)^{1/4}]\ln\left\{\frac{1}{2}[1+(1-e)^{1/4}]\right\}. \tag{36}$$

For $e>1$ indeed we have, obviously, $\sigma(e)=0$. This quantity is related to the Euler characteristic χ of the manifolds $M_e=\{\varphi|H(\varphi)\leqslant Ne\}$ (Ref. 30) and its singular behavior around the point $e=1$ is related to both the presence and the order of the phase transition that occurs.

In Fig. 3, the quantity σ is reported as a function of energy e: one can see that the presence of a phase transition is

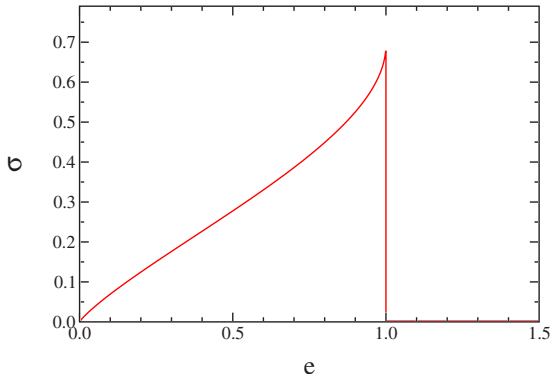

FIG. 3. (Color online) The entropy of saddles σ as a function of potential energy e.

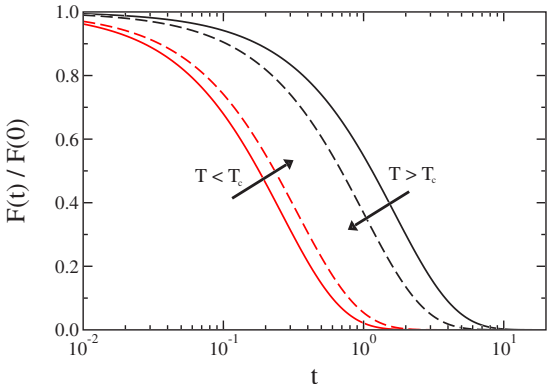

FIG. 4. (Color online) Time dependence of the self-correlation function $F(t)$ at different temperatures. From left to right: $T=0.1,0.5,0.6,1.0$ ($T_c=0.548$). Time is in normalized units.

signaled by a singularity of $\sigma(e)$ at the transition point $e=1$. It is worth noting that the curvature of the quantity $\sigma(e)$ around the transition point $e=1$ is positive, according to what was found in Ref. 30 for first-order transitions.

Summarizing, the study of stationary points shows that the presence of the phase transition is signaled by the stationary point properties. More specifically, the singular behavior of the configurational entropy $\sigma(e)$ at transition point $e=1$ is the topological counterpart of the thermodynamic transition: the topological hypothesis is verified for our model. We note, however, that these findings do not allow one to discriminate between the strong and weak topological hypotheses, as in this case the map M from equilibrium energy levels to stationary point energies is trivially the identity at the transition point $e=1$: $M(1)=1$.[46]

VI. COHERENCE PROPERTIES AND DYNAMICS

The dynamics of interacting lasing modes close to the mode-locking transition can also be investigated; it leads to explicit results for measurable correlation functions.

A. Single-mode first-order coherence

We start considering the single-mode ("self") first-order coherence:[47]

$$g_n^{(1)}(t) = \frac{\langle E_n^*(t_0)E_n(t_0+t)\rangle}{\langle E_n^*(t_0)E_n(t_0)\rangle}, \tag{37}$$

where $E_n(t)=\sqrt{\omega_n}a_n \exp(-i\omega_n t)$ is the electric field emitted at the angular frequency ω_n (omitting an inessential factor depending on the point in space where the field is measured). For quenched amplitudes, $\omega_n A_n^2 \cong \omega_0 A^2$, one has (omitting the mode index n)

$$g^{(1)}(t) = \frac{F^{(1)}(t)}{F^{(1)}(0)} e^{-i\omega_0 t}, \tag{38}$$

where $F^{(1)}(t)$ is the unnormalized single-mode first-order coherence given by

$$F^{(1)}(t) = \langle e^{i\varphi(t)} e^{-i\varphi(0)}\rangle, \tag{39}$$

and we used the fact that at equilibrium, the time average over t_0 can be replaced by a statistical average.[47] Below the threshold ($T>T_c$), the phases are uniformly distributed in $[0,2\pi)$, so that $F^{(1)}(t\to\infty)=0$. In contrast, at mode locking, the phase is blocked around a fixed value, thus $F^{(1)}(t\to\infty)\neq 0$.

We are interested in the time-delay profile of coherence function given by

$$F(t) = F^{(1)}(t) - F^{(1)}(\infty). \tag{40}$$

$F(t)$ can be explicitly calculated in the mean-field theory (see Ref. 46 for all the details of the computation). In fact, it can be shown that the single-mode dynamics can be mapped into the effective equation

$$\gamma\dot{\varphi}(t) = -4\zeta^3 \sin\varphi(t) + \eta(t), \tag{41}$$

where ζ is the thermodynamic value of the magnetization we determined in Sec. (4), η a δ-correlated Gaussian noise with variance $2\gamma T$, and γ a constant fixing the time scale (in the following, we use units such that $\gamma=1$).

From Eq. (41), it is evident that in the paramagnetic phase ($\zeta=0$), the phases will freely diffuse, while in the ordered (mode-locked) phase, they fluctuate around a given value that, without loss of generality, can be taken as $\varphi=0$. Equation (41) can be solved and the self-correlation function of a single mode,

$$F(t) = \langle e^{i\varphi(t)} e^{-i\varphi(0)}\rangle - \langle e^{i\varphi(t)}\rangle\langle e^{-i\varphi(0)}\rangle, \tag{42}$$

can be computed.[46] Using symmetry properties, the above function can be written as

$$F(t) = F_c(t) + F_s(t), \tag{43}$$

where

$$F_c(t) = \langle \cos\varphi(t)\cos\varphi(0)\rangle - \langle \cos\varphi(t)\rangle\langle\cos\varphi(0)\rangle,$$

$$F_s(t) = \langle \sin\varphi(t)\sin\varphi(0)\rangle. \tag{44}$$

Following Ref. 46, the self-correlations in Eq. (44) can be numerically determined and they turn out to be nearly exponential at all temperatures, $F_c(t)\propto e^{-t/\tau_c}$ and $F_s(t)\propto e^{-t/\tau_s}$. In Fig. 4, the function $F(t)/F(0)$ is shown for different temperatures. Upon increasing T, the decorrelation time increases for

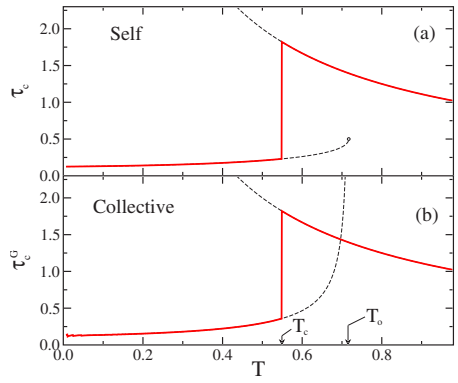

FIG. 5. (Color online) (a) Relaxation time τ_c of the self-correlation function $F_c(t)$ as a function of T. Full line corresponds to stable state (paramagnetic above T_c and ferromagnetic below it). Dashed lines refer to unstable solutions. (b) Relaxation time τ_c^G of the collective correlation function $G_c(t)$ as a function of T. Full and dashed lines are the same as in (a).

$T<T_c$, while it decreases for $T>T_c$ (after a sudden jump at T_c). This behavior is evident when analyzing the T dependence of the relaxation time. In the upper panel of Fig. 5, the quantity τ_c is shown as a function of temperature. Full lines refer to stable states, while dashed lines to unstable ones. We note that in paramagnetic high-T phase, τ_c (and τ_s) have a $1/T$ dependence, as expected for free Brownian motion. In the low-T phase, the behavior of τ_s (not shown in the figure) is very similar to that of τ_c.

Summarizing, in the absence of mode locking, the single-mode first-order coherence function has an exponential trend (corresponding to a Lorentzian linewidth), whose relaxation time decreases as the average energy per mode is reduced (i.e., the temperature is increased). At the mode-locking transition, the coherence function is expressed as the sum of two exponentials (corresponding to the two quadratures of the phase-modulated laser signal), whose time constants have a jump with respect to the free-run regime, and decreases while increasing the average energy per mode (and hence reducing the temperature).

B. Multimode first-order coherence

Here, we consider the multimode ("collective") first-order coherence:

$$g^{(1)}(t) = \frac{\langle E^*(t_0)E(t_0+t)\rangle}{\langle E^*(t_0)E(t_0)\rangle}, \tag{45}$$

with $E(t)=\Sigma_n\sqrt{\omega_n}a_n\exp(-i\omega_n t)$. In the quenched amplitude approximation, proceeding as above, it is possible to write

$$g^{(1)}(t) = \frac{G^{(1)}(t)}{G^{(1)}(0)}e^{-i\omega_0 t}, \tag{46}$$

where we have taken $\omega_n \cong \omega_0$ (since all the modes are taken as densely packed around ω_0, small differences between ω_n and ω_0 can be embedded in the phase φ_n), and

$$G^{(1)}(t) = \frac{1}{N^2}\sum_{nm}\langle e^{i\varphi_n(t)}e^{-i\varphi_m(0)}\rangle = \langle z(t)z^*(0)\rangle \tag{47}$$

is the correlation function of the magnetization $z(t)=N^{-1}\Sigma_n \exp[i\varphi_n(t)]$. We can write

$$G^{(1)}(t) = G^{(1)}(\infty) + \frac{1}{N}G(t) = \zeta^2 + \frac{1}{N}G(t), \tag{48}$$

where $G^{(1)}(\infty)=\zeta^2$ is the asymptotic value (we recall that $\zeta=\langle z\rangle$ is assumed real), which is acquired at the mode-locking transition, and the collective *connected* correlation function $G(t)$ is defined as

$$G(t) = N[G^{(1)}(t) - G^{(1)}(\infty)]$$
$$= \frac{1}{N}\sum_{nm}[\langle e^{i\varphi_n(t)}e^{-i\varphi_m(0)}\rangle - \langle e^{i\varphi_n(t)}\rangle\langle e^{-i\varphi_m(0)}\rangle]. \tag{49}$$

This function has a finite limit for $N\to\infty$ (see the Appendix), which can be computed following Ref 46. As for $F(t)$, $G(t)$ can be written as a sum of two terms,

$$G(t) = G_c(t) + G_s(t), \tag{50}$$

with

$$G_c(t) = \frac{1}{N}\sum_{nm}[\langle\cos\varphi_n(t)\cos\varphi_m(0)\rangle - \langle\cos\varphi_n(t)\rangle\langle\cos\varphi_m(0)\rangle],$$

$$G_s(t) = \frac{1}{N}\sum_{nm}[\langle\sin\varphi_n(t)\sin\varphi_m(0)\rangle\ . \tag{51}$$

Again, one finds an exponential decay, $G_c(t)\propto e^{-t/\tau_c^G}$ and $G_s(t)\propto e^{-t/\tau_s^G}$.[46] In the lower panel of Fig. 5, the relaxation time τ_c^G is shown as a function of temperature. We hence expect a trend for $G(t)$ which resembles $F(t)$; however, it is worth noting that the quantity τ_c^G diverges when $T\to T_o^-$, that is, when, starting from low-T phase, the point where the unstable solution (dashed line) disappears is approached. The occurrence of the thermodynamic transition at $T_c<T_o$ prevents the divergence of τ_c^G. The τ_s^G (not shown) does not diverge at T_o.

C. Multimode second-order coherence

We also consider the multimode (collective) second-order coherence:

$$g^{(2)}(t) = \frac{\langle E^*(t_0)E^*(t_0+t)E(t_0)E(t_0+t)\rangle}{\langle E^*(t_0)E(t_0)\rangle^2} = \frac{\langle I(t_0)I(t_0+t)\rangle}{\langle I(t_0)\rangle^2}, \tag{52}$$

again with

$$E(t) = \sum_n \sqrt{\omega_n}a_n e^{-i\omega_n t} \propto z(t)e^{-i\omega_0 t}. \tag{53}$$

We get

$$g^{(2)}(t) = \frac{G^{(2)}(t)}{G^{(2)}(\infty)}, \tag{54}$$

where $G^{(2)}(t) = \langle z(t)z^*(t)z(0)z^*(0)\rangle$. We can decompose this function in its connected components [see Eq. (4.23) Ref. 48]. Recalling that $\zeta = \langle z\rangle$ is assumed real, we get

$$G^{(2)}(t) = \langle z(t)z^*(t)z(0)z^*(0)\rangle_c + \zeta G_3(t) + \langle z(0)z^*(0)\rangle_c^2 + |\langle z(t)z(0)\rangle_c|^2 + |\langle z(t)z^*(0)\rangle_c|^2 + \zeta^4, \tag{55}$$

where the function $G_3(t)$ is a sum of connected three-point functions: $G_3(t) = 2\,\mathrm{Re}[\langle z(t)z^*(t)z(0)\rangle_c + \langle z(t)z(0)z^*(0)\rangle_c]$. Using the results of the Appendix, we have $\langle z(t)z^*(t)z(0)z^*(0)\rangle_c \propto N^{-3}$ and $G_3 \propto N^{-2}$; from Eqs.(49) and (51), we have

$$\langle z(0)z^*(0)\rangle_c = N^{-1}G(0),$$

$$\langle z(t)z(0)\rangle_c = N^{-1}[G_c(t) - G_s(t)],$$

$$\langle z(t)z^*(0)\rangle_c = N^{-1}[G_c(t) + G_s(t)]. \tag{56}$$

Then, we obtain

$$G^{(2)}(t) = \zeta^4 + \frac{G(0)^2 + 2G_c(t)^2 + 2G_s(t)^2}{N^2} + \zeta G_3(t) + O(N^{-3}). \tag{57}$$

In the paramagnetic phase, $\zeta = 0$, and by symmetry $G_s(t) = G_c(t) = G(t)/2$; moreover, these functions tend to 0 for $t \to \infty$. Then, we get

$$g^{(2)}(t) = \frac{G(0)^2 + 2G_c(t)^2 + 2G_s(t)^2}{G(0)^2} = 1 + \frac{G(t)^2}{G(0)^2} = 1 + |g^{(1)}(t)|^2, \tag{58}$$

where we also make use of Eq. (48). This result is indeed what we expect for light modes evolving independently and rapidly.

In the mode-locked phase, Eq. (58) will not hold but a relation between $g^{(2)}$ and $g^{(1)}$ can still, in principle, be deduced from the knowledge of function $G_3(t)$, using Eqs. (57) and (48). Future works will address this point.

VII. CONCLUSIONS

By using a simple model that is expected to describe multimode dynamics of tightly packed extended and/or localized modes in a nano-optical resonator, we predict the existence of a first-order phase-locking transition when the averaged energy per mode is above a critical value (correspondingly, the adimensional effective temperature is below T_c). This value depends on the average value of the mode-overlap coefficient g. If the transition involves extended modes, one has (omitting indexes) $g \cong \omega_0^2 \int |E|^4 dV \cong \chi_0 \omega_0^2 V^{-1}$, with χ_0 a reference susceptibility value. Conversely, if localized modes are involved, it is $g \cong \chi_0 V_0^2 \omega_0^2$, where V_0 is the average localized mode volume ($V_0 \propto L_0^2$ with L_0 the localization length). In the former case, for a fixed spontaneous emission noise T_{bath}, it is found that the critical mean energy per mode is V dependent,

$$\mathcal{E}_c^{(ext)} = \omega_0 A^2 = \sqrt{\frac{k_B T_{bath} V}{T_c \chi_0}}, \tag{59}$$

while for localized modes

$$\mathcal{E}_c^{(loc)} = \omega_0 A^2 = \sqrt{\frac{k_B T_{bath} L_0^3}{T_c \chi_0}}. \tag{60}$$

Hence, the critical energy for the phase-locking transition has very different scaling behavior with respect to the system size, depending on the degree of localization of the involved modes. In the general case, one can expect intermediate regimes between those considered, so that the trend of the critical energy (determined by the amount of energy pumped in the system per unit time, i.e., the pumping rate) versus system volume is an interesting quantity which can be experimentally investigated. A topology-thermodynamics relationship has been evidenced for our model, corroborating previous findings on this topic: the thermodynamic transition is signaled by a singularity in the topological quantity σ.

The exact solution of the dynamics of the model predicts the divergence of the relaxation time of the first-order coherence function $g^{(1)}$ at the transition. This behavior might be observed in experiments; the different scaling with respect to the system size also affects the position of the transition, as determined by the predicted jump in the relaxation time or, equivalently, in an abrupt change of the single-mode laser linewidth while varying the pumping rate.

This analysis points out the rich phase-space structure displayed by these systems, while varying the amount of disorder or the profile of the density of states. Hence, nanolasers not only may furnish the basis for highly integrated short-pulse generators, but are a valuable framework for fundamental physical studies. These deserve future theoretical and experimental investigations and can be extended to other nonlinear multimode interactions.

APPENDIX

We discuss here the scaling of the correlations of z when $N \to \infty$. The basic fact is that the variable z is intensive and, for a mean-field system, has a probability distribution of the form[48]

$$P_N(z) = e^{NF(z)}, \tag{A1}$$

where F is related to the thermodynamic free energy of the system. Consider the generating functional

$$e^{NF(j)} = \langle e^{Njz}\rangle = \int dz e^{N[F(z)+jz]}, \tag{A2}$$

then for large N, $F(j) = \max_z[F(z) + jz]$ and it is a quantity of order 1. The *connected correlation functions*[48] are derivatives of $NF(j)$ with respect to Nj:

$$\langle z^k\rangle_c = \left.\frac{\delta^k NF(j)}{(\delta N j)^k}\right|_{j=0} = N^{1-k}\left.\frac{\delta^k F(j)}{(\delta j)^k}\right|_{j=0}. \quad \text{(A3)}$$

This simple argument shows that $\langle z^k\rangle_c \propto N^{1-k}$. In particular,

$$\langle z^2\rangle_c = \langle z^2\rangle - \langle z\rangle^2 \propto N^{-1},$$

$$\langle z^3\rangle_c = \langle z^3\rangle - 3\langle z\rangle\langle z^2\rangle_c - \langle z\rangle^3 \propto N^{-2},$$

$$\langle z^4\rangle_c = \langle z^4\rangle - 4\langle z\rangle\langle z^3\rangle_c - 3\langle z^2\rangle_c^2 - \langle z\rangle^4 \propto N^{-3}. \quad \text{(A4)}$$

We assumed that z is real but the same derivation can be repeated for a complex variable; the only difference is in the definition of the connected correlation functions.

For the dynamics, one can write a similar expression for the probability of a trajectory $z(t)$ (see Ref. 46 and references therein):

$$P_N[z(t)] = e^{NF[z(t)]}. \quad \text{(A5)}$$

Repeating the derivation above using functional integrals, one obtains exactly the same results for the scaling with N.

[1] A. Yariv, *Quantum Electronics* (Saunders College, San Diego, 1991).
[2] A. E. Siegman, *Lasers* (University Science Books, Sausalito, CA, 1986).
[3] H. A. Haus, IEEE J. Quantum Electron. **6**, 1173 (2000).
[4] J. D. Joannopoulos, P. R. Villeneuve, and S. Fan, *Photonic Crystals* (Princeton University Press, Princeton, 1995).
[5] K. Sakoda, *Optical Properties of Photonic Crystals* (Springer-Verlag, Berlin, 2001).
[6] Y. Liu, Z. Wang, M. Han, S. Fan, and R. Dutton, Opt. Express **13**, 4539 (2006).
[7] H. Haken, *Synergetics* (Springer-Verlag, Berlin, 1978).
[8] F. Papoff and G. D'Alessandro, Phys. Rev. A **70**, 063805 (2004).
[9] E. Cabrera, M. Sonia, O. G. Calderon, and J. M. Guerra, Opt. Lett. **31**, 1067 (2006).
[10] A. Gordon and B. Fischer, Phys. Rev. Lett. **89**, 103901 (2002).
[11] A. Gordon and B. Fischer, Opt. Commun. **223**, 151 (2003).
[12] J. Sierks, T. J. Latz, V. M. Baev, and P. E. Toschek, Phys. Rev. A **57**, 2186 (1998).
[13] P. G. De Benedetti and F. H. Stillinger, Nature (London) **410**, 259 (2001).
[14] D. Wales, *Energy Landscapes* (Cambridge University Press, Cambridge, 2004).
[15] L. Angelani, R. Di Leonardo, G. Ruocco, A. Scala, and F. Sciortino, Phys. Rev. Lett. **85**, 5356 (2000).
[16] C. Conti, Phys. Rev. E **72**, 066620 (2005).
[17] C. Conti, M. Peccianti, and G. Assanto, Opt. Lett. **31**, 2030 (2006).
[18] L. Angelani, C. Conti, G. Ruocco, and F. Zamponi, Phys. Rev. Lett. **96**, 065702 (2006).
[19] L. Angelani, C. Conti, G. Ruocco, and F. Zamponi, Phys. Rev. B **74**, 104207 (2006).
[20] R. Gilmore, *Catastrophe Theory for Scientists and Engineers* (Dover, New York, 1981).
[21] L. Caiani, L. Casetti, C. Clementi, and M. Pettini, Phys. Rev. Lett. **79**, 4361 (1997).
[22] L. Casetti, M. Pettini, and E. Choen, Phys. Rep. **337**, 237 (2000).
[23] R. Franzosi and M. Pettini, Phys. Rev. Lett. **92**, 060601 (2004).
[24] R. Franzosi, M. Pettini, and L. Spinelli, arXiv:math-ph/0505057 (unpubished).
[25] R. Franzosi and M. Pettini, arXiv:math-ph/0505058 (unpublished).
[26] L. Casetti, M. Pettini, and E. G. D. Cohen, J. Stat. Phys. **111**, 1091 (2003).
[27] M. Kastner, Phys. Rev. Lett. **93**, 150601 (2004).
[28] P. Grinza and A. Mossa, Phys. Rev. Lett. **92**, 158102 (2004).
[29] A. C. Ribeiro Teixeira and D. A. Stariolo, Phys. Rev. E **70**, 016113 (2004).
[30] L. Angelani, L. Casetti, M. Pettini, G. Ruocco, and F. Zamponi, Europhys. Lett. **62**, 775 (2003).
[31] M. Kastner, arXiv:cond-mat/0703401 (unpublished).
[32] W. E. Lamb, Phys. Rev. **134**, A1429 (1964).
[33] I. C. L. O'Bryan and I. M. Sargent, Phys. Rev. A **8**, 3071 (1973).
[34] The coupled-mode equations (1) can be viewed as generalized "self-trapping" equations (Ref. 35) in the imaginary-time domain including thermal noise.
[35] J. C. Eilbeck, P. S. Lomdahl, and A. C. Scott, Physica D **16**, 318 (1985).
[36] P. Meystre and M. Sargent III, *Elements of Quantum Optics* (Springer, Berlin, 1998).
[37] W. Brunner and H. Paul, Opt. Quantum Electron. **15**, 87 (1983).
[38] S. Mujumdar, M. Ricci, R. Torre, and D. S. Wiersma, Phys. Rev. Lett. **93**, 053903 (2004).
[39] K. L. van der Molen, R. W. Tjerkstra, A. P. Mosk, and A. Lagendijk, Phys. Rev. Lett. **98**, 143901 (2007).
[40] X. Wu, J. Andreasen, H. Cao, and A. Yamilov, arXiv:physics/0701193 (unpublished).
[41] S. John, Phys. Rev. Lett. **58**, 2486 (1987).
[42] L. Angelani, L. Casetti, M. Pettini, G. Ruocco, and F. Zamponi, Phys. Rev. E **71**, 036152 (2005).
[43] L. Angelani, G. Ruocco, and F. Zamponi, J. Chem. Phys. **118**, 8301 (2003).
[44] A. Andronico, L. Angelani, G. Ruocco, and F. Zamponi, Phys. Rev. E **70**, 041101 (2004).
[45] L. Angelani, G. Ruocco, and F. Zamponi, Phys. Rev. E **72**, 016122 (2005).
[46] F. Zamponi, L. Angelani, L. Cugliandolo, J. Kurchan, and G. Ruocco, J. Phys. A **36**, 8565 (2003).
[47] R. Loudon, *The Quantum Theory of Light*, 2nd ed. (Clarendon, Oxford, 1983).
[48] G. Parisi, *Statistical Field Theory* (Academic, New York, 1998).